Sediment Transport, Artisanal Gold Mining, and the Evaluation of Potential Mercury Contamination in Madre de Dios, Peru

Axel Berky
Dr. Marco Marani and Dr. Bill Pan, Advisors
May 2014

Masters project submitted in partial fulfillment of the requirements for the Master of Environmental Management degree in the Nicholas School of the Environment of Duke University

2014

Table of Contents

Acknowledgements

This project would not been possible without the use of publically available ASTER Global DEM and MODIS data. I would like to accredit NASA LP DAAC for the invaluable data that it provided. ASTER data is a product of METI and NASA and is supported by NASA's Earth Science Data Systems Program.

I would like to thank my advisors Marco Marani and William Pan for the opportunity to work on such an interesting project as well as for all of their continued support and guidance. This project would have not been possible without them. I would also like to thank the Bass Connections team, the Peruvian Ministry of the Environment as well as John Terborgh for providing essential data and documents. Lastly, I dedicate this work to my grandfather, Mauricio André.

Abstract

In the last several decades, artisanal mining in Madre de Dios, Peru has grown at an exponential rate. The lack of regulation of mining practices and the use of mercury in the gold extraction process has culminated in a human and environmental health risk. Mining practices in Madre de Dios have led to deforestation as well as detrimental health effects in humans. It has also led to mercury contaminated soil that is then transported downriver. This study uses mathematical modeling and geographic information systems (GIS) to better understand sediment transport and quantify potentially contaminated soil transport through a detachment model for the entire Madre de Dios watershed. The model considers spatially-distributed rainfall, leaf area index, topographic slope, and grain size and determines the spatial patterns of sediment erosion and deposition.

The model estimates that erosion has increased 13.1tons/km2/year due to artisanal gold mining, demonstrating that it has had a notable impact at the whole-watershed scale. However, the environmental impact on the sub-watershed of Huepetuhe, where much of the gold mining is occurring, is even more substantial, with an additional 840,175 tons/year of sediment being eroded from the areas most affected by mercury contamination. Most of this erosion consists of finer grain sizes that are associated with natural mercury levels and the ability to transport adsorbed mercury. The results overall suggest that mercury from natural or anthropogenic sources could be readily transported downriver and provide indications as to where the resulting mercury contamination may be more severe.

Introduction

Recent studies have shown that artisanal gold mining in the Department of Madre de Dios, Peru has had deleterious impacts on environmental and human health through the exposure to and release of mercury. These impacts have increased drastically as artisanal gold mining has grown exponentially over the last several decades due to the rising price of gold on the world market. Understanding the mining process as well as the many social and environmental factors associated with artisanal gold mining in the region are crucial in comprehending and improving human and environmental health in Madre de Dios.

Mining in Madre de Dios usually occurs on the riverbanks, where sediments are dredged and are passed over a sieve, allowing the finer grains to be collected. Other practices use high powered hoses to erode the banks of the river to obtain fine sediment. A recently passed law has made it illegal for mining to occur on the river. In response, miners have established mines slightly inland in which a trench is dug to connect the mine to a nearby river. The area is deforested and high powered hoses are used to erode the landscape. Once the fines grains are gathered, they are then mixed by hand with elemental mercury to extract the small flecks of gold that are present in the soil. This is due to mercury's affinity to readily bind to gold and form a mercury-gold amalgam that is then easily extracted from the sediment. The amalgam is then burned in order to volatilize the mercury, leaving the gold. In this process, people are able to absorb up to 80% of the volatilized mercury via inhalation and are statistically shown to have higher mercury levels compared to the rest of the population (Yard, 2012). The mercury is often burned off in small mining towns such as Huepetuhe and Boca Colorado; however, it may also be done at the mining camp. These practices fail to use personal protective equipment and cause direct elemental mercury exposure to humans via dermal contact as well as respiration (Swenson, 2010).

Once in its gaseous state, mercury can be transported long distances and be deposited on the Earth's surface by deposition or via rainfall. This natural deposition provides a background level of mercury in the region; however, background levels and the extent of deposition is not well known. A Peruvian report states that the extent to which volatilized mercury from gold mining is able to be transported is partially dependent on humidity and may not be transported more than several kilometers (Alvarez, 2011). This entails that mercury vapor could travel from the gold processing shops in mining communities to other parts of town and adversely affect susceptible populations such as young children.

The evaluation of mercury contamination is especially complex due to the many forms that it can possess. Mercury contamination of river sediment poses a high risk to human and environmental health as bacteria living in the sediment can methylate elemental mercury, making it more bioavailable and able to bio-magnify in the food chain. The bio-magnification of methylmercury can lead to high levels of mercury contamination in fish tissues, which is a common food source for many people living in the region. Methylmercury is a known neurotoxin and can cause developmental problems such as learning disorders, memory deficiency, and neurological disorders in children (Zahir, 2005). A study by Katy Ashe demonstrated a correlation between fish consumption and mercury levels in people living in Madre de Dios, with a portion of the population having harmful levels of mercury (Ashe, 2012). Another study conducted in the mining town of Huepetuhe showed that people who ate more fish had statistically significant higher mercury levels than those who ate less fish (Yard, 2012).

The health impact from artisanal gold mining has the potential to impact entire communities. A study on 103 of the residents of Huepetuhe demonstrated that all residents had elevated mercury levels, ranging from 0.7µg/g creatinine to 151µg/g creatinine in urine, which is representative of inhalation exposure (Yard, 2012). Although there is relatively little data on the exposure level of mercury needed to incite clinical symptoms, available data suggests that as little

as 10µg/g may cause impairments in the nervous system (Lucchini, 2002). Higher levels ranging from 30µg/g to 100µg/g have been shown to result in psychological disorders, tremors and an impaired nervous system (Kazantzis, 2002). Of the town members tested, 91.3% had detectable levels of methylmercury in their blood that ranged from 6µg/L Hb to 10µg/L Hb. Community members also reported health conditions such as digestive disorders, kidney dysfunction and nervous system disorders. Although such an in-depth study has only been done in Huepetuhe, similar results could be found in other small mining towns (Yard, 2012). The accumulating evidence of the adverse health effect from mercury exposure validate that artisanal gold mining in Madre de Dios has a detrimental impact on human health.

Beyond adversely affecting human health, artisanal gold mining is also the main driver of deforestation in the region. The Huepetuhe, Guacamayo, and Delta 1 are all mines that are easily visible in satellite imagery and have greatly increased in size over the last two decades as shown in a recent study by Asner et al. (2013), Figure 1.

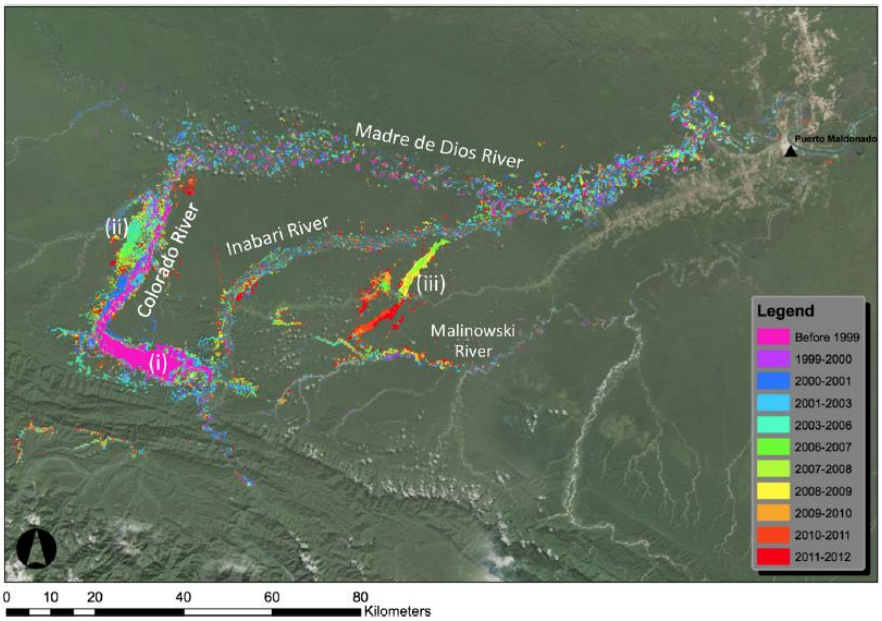

Fig. 2. The regional extent and occurrence of small and large mines throughout the southern Madre de Dios region. Note that many mines are closely situated through time, and thus the color chart may not show the year of every mining event. See Figs. S1–S3 for detail. Location key: (*i*) Huepetuhe, (*ii*) Delta-1, (*iii*) Guacamayo. All other unlabeled mines are in the "small mine" category as described throughout the artide.

Figure 1: Mining sites in Madre de Dios the year initiated. Taken from Asner, 2013.

A study by Jennifer Swenson et al. demonstrated that mining sites in Madre de Dios have grown substantially from 2003 and 2009 with an annual growth of 220ha/yr. This increase in gold mining has been shown to be dependent on the global market price of gold. Peruvian mercury imports have also increased proportionally with the global price of gold and were around 500 tons per year until 2010 (Swenson, 2010). Much of this mercury is used in artisanal gold mining and is potentially released into the environment through unregulated mining practices. The Madre de Dios region is estimated to produce 16,000 kg of gold a year, each of which is believed to require 2.8 kg of mercury. This entails that an approximate 44,800 kg of mercury per year could be released into the environment through artisanal gold mining (Alvarez, 2011).

The possibility to gain economic stability has caused an increasing number of people from various cities in Peru to migrate to Madre de Dios to mine for gold. It is currently estimated that there are over 30,000 miners in Madre de Dios; however, the actual number is unknown as miners do not register with the local government. If gold prices continue to rise, it is likely that levels of mercury released in Madre de Dios will continue to rise as well. This makes artisanal gold mining a potentially escalating problem as more Peruvians migrate to the region to seek economic stability.

While it is acknowledged that the social and environmental impact of gold mining is substantial, data on actual mercury concentrations in the Madre de Dios region are limited. A recent research brief released last month by the Carnegie Institution for Science measured levels of mercury in fish tissue and human hair; however, as of yet no data on mercury concentrations in suspended or deposited sediment in Madre de Dios have been published. There is also very little data on the hydraulic properties of the Madre de Dios River (Thieme, 2007). A study on the Madeira River, to which the Madre de Dios River is a tributary, demonstrated that the majority of the suspended sediment consisted of silt ranging between 7 – 13μm in diameter (Guyot, 1999).

Mercury concentrations bound to sediment and the overall sediment transport within the Madre de Dios is important as mercury can be transported via sediment. Mercury has a strong affinity to small clay particles since they have a larger surface area to volume ratio and are less stable, meaning they are more likely to form bonds (Miller, 2007). While mercury contamination in the region is expected to be from artisanal gold mining, as in other Amazonian regions, mercury naturally found in the soil may be an important source of mercury (Forsberg, 1999). Soil samples taken along the Madiera River in alluvial terraces, downstream from Porto Velho in Brazil found mercury concentrations that ranged from 232 to 406ng/g, while upland soils were found to have mercury concentrations ranging from 245 to 439ng/g (Lechler, 2000). Other soils sampled from areas removed from gold mining but in the same region of Porto Velho, in the Rio Negro Basin, were measured to have mercury levels up to 212ng/g Hg (Forsberg, 1999) with an average of 164ng/g (Jardim, 1998). Although these studies are from different regions of the Amazon basin, a similar scenario may be occurring in the Madre de Dios Watershed. While this does not negate the large quantities of mercury that mining is introducing into the environment, deforestation as well as the anthropogenic erosion from gold mining may also be contributing to mercury contamination in the region.

Quantifying soil erosion in Madre de Dios will provide important information about naturally occurring geomorphological processes and the extent to which they are being impacted by artisanal gold mining. It may also provide support for the growing theory that Amazonian soils are an important source of mercury contamination. Once an estimate for erosion is established, a better understanding of sediment transport and discharge can be obtained. Modeling sediment transport, especially for finer grains, could aid in locating potential hotspots of mercury contamination, which would be important sites for future studies. These factors make the modeling of erosion and sediment transport in the Madre de Dios basin important for determining current as well as prospective impacts of artisanal mining on human and environmental health in Madre de Dios.

Objective

The project's main objective is to apply a global soil detachment model introduced by Jon Pelletier that is able to quantify soil erosion and apply it to the Madre de Dios Watershed (Pelletier, 2011). His original model quantified sediment detachment based on four main variables: leaf area index, precipitation, rainfall and slope. This will provide important information on how gold mining is impacting soil erosion as well as sediment transport in a region where limited data is available. The second objective is to identify hotspots for erosion in the watershed and determine their potential impact as well as how they have changed before and after artisanal gold mining. The third objective is to determine areas in which sediment will become deposited to aid in determining locations where future sampling should be conducted.

Study Area

The Madre de Dios Watershed is located in the department of Madre de Dios, Peru which resides in the South Eastern Peruvian Amazon, bordering Bolivia, and has the lowest population density in Peru (Figure 2). The department is 85,300 km^2 or approximately the size as the state of Indiana. The majority of the region is comprised of tropical rain forests. Lowland mountains are also present in the Southwestern region of the department and are part of the Andes mountain range. Two national parks, Manu and Tambopata, as well as a communal reservation, Amarakaeri, have also been established to help preserve the great biodiversity in the region, which is known to be one of the most diverse ecosystems in the world (Brooks, 2006). Puerto Maldonado, the department's capital, is the largest city in the region with a total population of 210,000. While other small towns exist, their populations and sizes are much smaller than the department's capital.

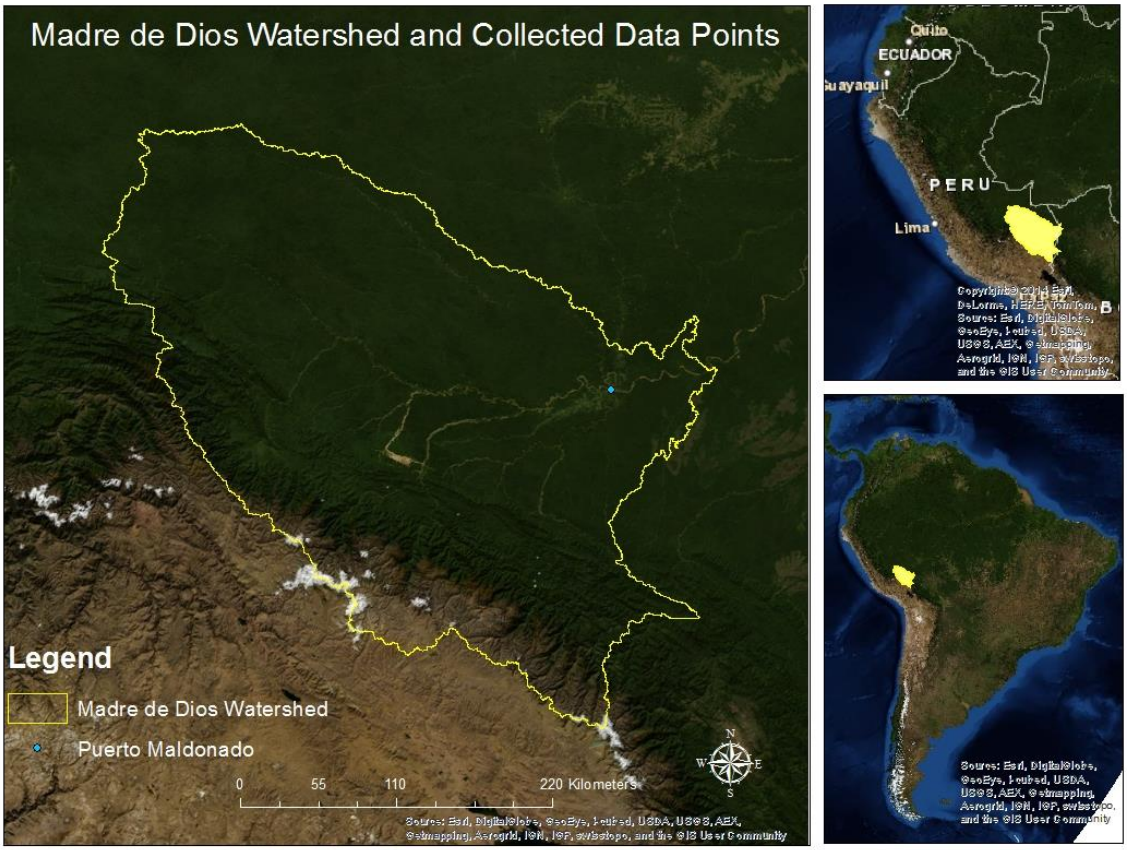

Figure 2: Geographic location of the Madre de Dios watershed and the department's capital city, Puerto Maldonado.

Modeling Methods

Due to the lack of data, including discharge, daily precipitation, river depth, and site specific soil data, only a rudimentary model can be designed to better understand soil erosion as well as sediment transport in the Madre de Dios Watershed and its influence on the Madre de Dios River. To do this, a large-scale model proposed by Jon Pelletier was applied that determines soil erosion based on geographic coordinates (x, y) as well as grain size (d). The model inputs consist of mean monthly rainfall (R), slope (S), mean monthly leaf area index (LAI) (L), soil fraction (f_d) for each grain size and bulk density (ρ_b), which are related to the yearly detachment rate by

$$(x, y, d) = c_1 \rho b \, f d \, S^{5/4} \sum_{k=1\ldots12} Rke^{-Lk}$$

where k spans the twelve months of the year. The variable c_1 is a free parameter and was determined by Pelletier by trial and error until model results obtained the minimum sum of square differences when compared to global datasets. On a global scale, c_1 was determined to equal 0.15. Due to a lack of sediment discharge data for the Madre de Dios Watershed, the global value was originally used. With these inputs, the model generates the yearly sediment erosion rate (or detachment rate, $kg/m^2/yr$) for each soil type (sand, silt, clay) at every pixel in the watershed. These detachment rate values are then used in a sediment transport model. The model starts at the highest elevation in the watershed and proceeds from one pixel to the next following the trajectory of the steepest path to simulate hydrological transport processes. Whether or not sediment is transported depends on the Rouse number, which is a function of settling velocity, W_s, depth, and slope (Ferguson, 2004). Settling velocity values of sand, silt, and clay were determined by a study from Ferguson (2004) and were measured to be 0.011, .006 and .00425, respectively. Rouse numbers below the critical threshold (Rc) of 1.2 indicate that suspended load transport is possible, while higher Rouse numbers indicate sediment becomes deposited or transported as bedload (if conditions allow). The critical value Rc thus distinguishes between sediment that is commonly transported via suspension in the water column and bed load sediment whose main transport is by rolling and saltation. The Rouse number was determined as follows (Pelletier, 2011):

$$R\# = \frac{Ws}{\kappa u^*}$$

Where

$$u^* = \sqrt{ghS}$$

However, due to the fact that shear velocity is assumed to have only a slight impact in comparison to slope, a simplified equation was implemented.

$$R\#(x, y, d) = c_2 \frac{Ws}{S^{1/2}}$$

Similar to c_1, c_2 is a free parameter that allows the model to obtain outputs with the lowest sum of the square difference compared to measured data. Since sediment yield in the Madre de Dios River has not been measured, the global scale value of 300s/m, as determined by Pelletier, was used here. Although the use of global scale parameters for c_1 and c_2 are not ideal, Pelletier's model obtained an R^2 value of 0.79 in representing measured sediment yield values for 128 rivers (including the Amazon river), supporting this choice.

Rainfall

The interpolation of rainfall in the Madre de Dios Watershed is one of the most important variables as it determines the quantity and geospatial location of water influxes throughout the region. Montlhy rainfall data, provided by the Peruvian Ministry of the Environment and John Torbergh (unpublished data), from 12 rainfall gauges were avaible and cover the entire Madre de Dios region, with one point in the far Northwest in Pasco, Peru (Perú Ministerio de Agricultura, 2010). Rainfall in the Madre de Dios basin was shown to be highly heterogeneous between rain gauges even in close proximity. A trend analysis on the rainfall data, Figure 3, shows that average yearly rainfall appears to steeply decrease from West to East, while a more gentle decrease is present from North to South. However, this North-South trend may be an artifact due to the location and lack of datapoints. There appears to be a strong relationship between precipitation and elevation in which a strong pulse in rainfall occurs aournd 800 meters above sea level (Figure 4). This pulse is likely associated with the strong orographic forcing caused by the Andes Mountains.

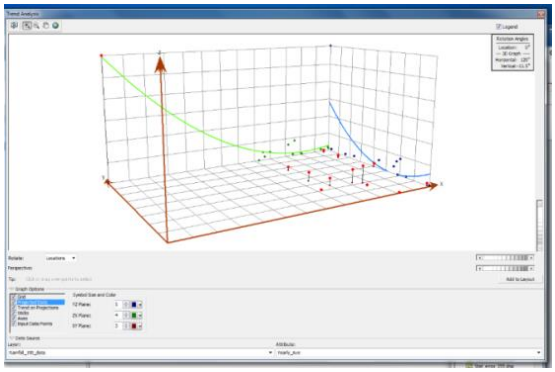

Figure 3. Trend analysis using ArcMap of yearly rainfall in Southeastern Peru.

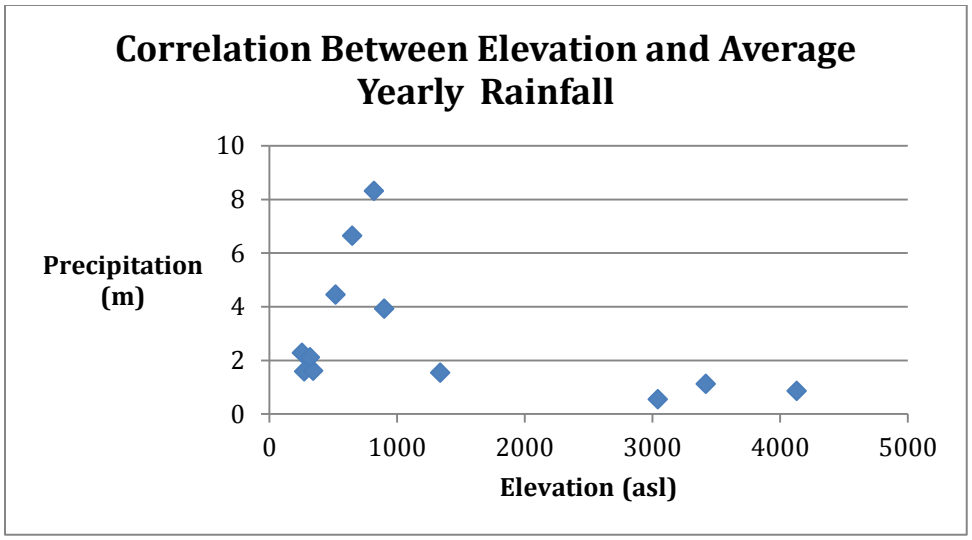

Figure 4: Scatterplot of rainfall and elevation, demonstrates a spike in rainfall at 820 meters above sea level.

While orographic forcing certainly depends on multiple variables, rather than just on elevation, the scatterplot in Figure 4 suggests that the more complex orographic effects in rainfall on the local regime can be surrogated by elevation alone, by assuming an increase in precipitation up to about 1,300m and an approximately constant mean at high elevations, above 1,300m. To interpolate rainfall, the rain gauges were split into two groups by elevation, with those at elevations higher than 1,300m in one group and rain gauges below 1,300m in another. A linear regression was used for gauges below 1,300m, Figure 5, while a constant mean was assumed for gauges above 1,300m. The residuals between rainfall observations with respect to the mean trends assumed above were then determined and interpolated using ordinary kriging. The mean value for each location was then added to yield the final interpolated value. The two interpolated regions were then combined together to produce the final interpolated surface.

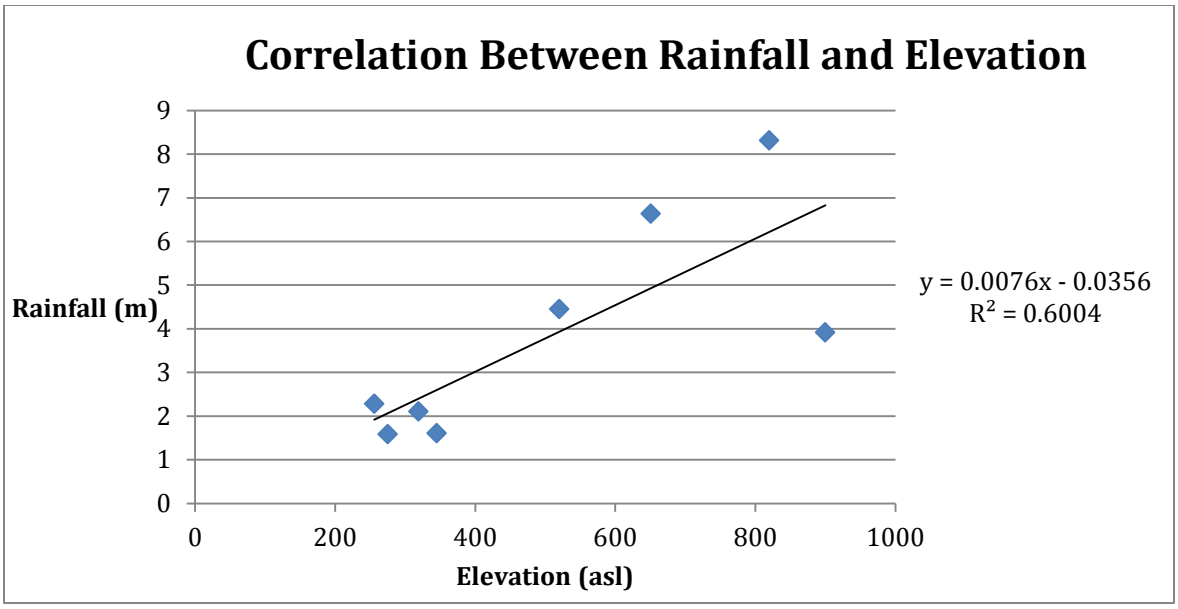

Figure 5: Scatterplot of rainfall and elevation, showing a high correlation between rainfall and elevation with an R^2 value of 0.6.

Leaf Area Index

LAI data was downloaded from MODIS MCD15A3, which is a composited image collected after 4 days of data collection and is provided at a one kilometer resolution (Knyazikhin, 1999). LAI values range from zero, bare ground, to 10 which represents a dense forest canopy. Given the location of the Madre de Dios Watershed in respect to the MODIS pathway, two MCD15A3 images were downloaded for each month. Dates of the images ranged from the 10th- 14th. For each month, the two downloaded images were merged together and re-projected in WGS 1984 UTM 19S (Appendix A). The downloaded MCD15A3 values were then converted into LAI values as seen in Figure 6. Since the images have a valid range of values from 0-100, this was condensed to 0-10 to correlate with maximum range of LAI values. MODIS values from 249-255 are classifications of various land types. In order to correct for these pixels, they were manually corrected and given a LAI value to reflect their land cover class.

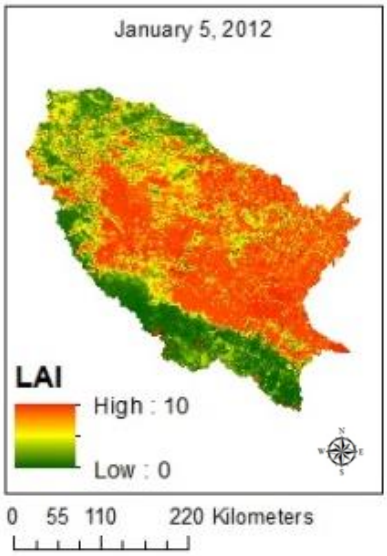

Figure 6: Final LAI values for the Madre de Dios Watershed in 2012.

Grain Size

Since no datasets were found that measured the grain size throughout the Madre de Dios Watershed, the Harmonized World Soil Database (HWSD) was used. The watershed was separated into 4 distinct zones, similar to the HWSD, starting from the lowest point of the Madre de Dios River. Each zone was given corresponding percent values of sand, silt and clay as established by the database. As seen in Table 1, most of the zones, especially those at higher elevations are comprised of sand. Zones at the lower elevations, zones 1 and 2, have substantial amounts of silt and clay. An example of the grain distribution is shown in Figure 7. The soil bulk density was also taken from the HWSD and was found to be 1300kg/m^2 (FAO, 2012).

Table 1: Percent grain composition for the four zones that comprise the Madre de Dios Watershed (FAO, 2012).

Zone	Sand (%)	Silt (%)	Clay (%)
1	50	30	20
2	13	61	26
3	61	23	10
4	83	9	8

.

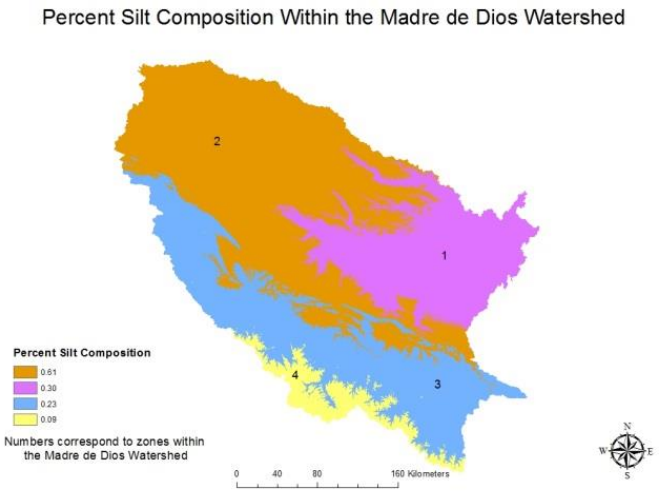

Figure 7: The percent silt composition within the 4 zones in the Madre de Dios Watershed (FOA, 2012).

Slope

The topography of the Madre de Dios Watershed was determined using ASTER digital elevation map (DEM) data, appendix B (NASA, 2001). This was then used to calculate slope, Figure 8. Since the vertical error of ASTER data can be up to several meters, slope was determined by using two methods based on the topography of the landscape. In areas with steep topography, slope was obtained by calculating the slope between pixels. This is because the error in elevation is minimal compared to the pixels difference in elevation. To minimize errors in slope in the Madre de Dios basin, the slope of pixels was determined by calculating change in elevation from the given pixel to the watershed's pour point. This corrected for any errors in the DEM for pixels with low slope values.

With these datasets and using the previously described equations a sediment detachment and transport model was developed for the Madre de Dios watershed. This model differs from Pelletier's as it uses a 30m resolution and incorporates rainfall data in the region to obtain a more spatially detailed understanding of erosion in the Madre de Dios basin.

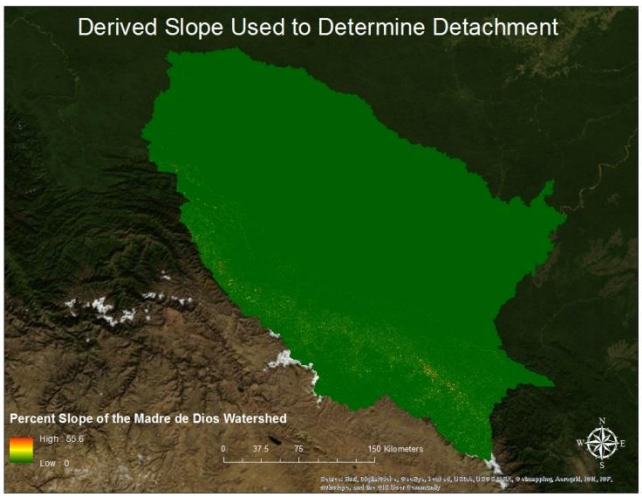

Figure 8: The resulting slope values for the Madre de Dios Watershed after correcting for areas of low differences in elevation.

Results

The Madre de Dios Watershed was found to comprise 92,263km^2 with a mean elevation of 3,119 meters (see Table 2). Its mean monthly rainfall is 290mm with an annual average of 2.5meters. The resulting interpolation of the yearly average rainfall, Figure 9, predicts that rainfall ranges from 1.0m to 11.3m and is highly dependent on elevation. This is due to the Andes Mountains being a main contributor to promoting rain events. Figure 9 also shows the location of the rain gauge stations used in the interpolation was well as the yearly average rainfall measured at each. The stations are represented as yellow points, while their size corresponds to the amount of rainfall recorded.

Table 2: Watershed Properties of the Madre de Dios Watershed.

Watershed Properties	
Basin Area (km$^{2)}$	92,263
Mean Elevation (m)	3,119
Mean Annual Rainfall (m)	2.5
Basin Relief Ratio (m/km)	21

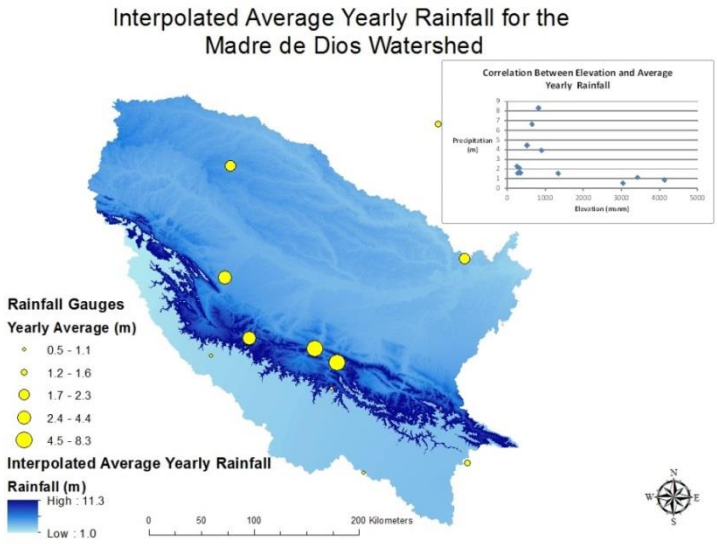

Figure 9: Rain gauges in Southeastern Peru and the resulting interpolated yearly rainfall for the Madre de Dios watershed.

While the model requires monthly LAI values, no such composite images were able to be downloaded; therefore four day composite images were use and demonstrate the impact of cloud cover on LAI. This can be seen in the month of January as the LAI values change drastically over a short period of time, Figure10. In 10a (Jan 1st), most of the LAI values are below 5, while four days later in 10b (Jan 5th) the majority of the watershed has LAI values above 5. This drastic change in LAI over such a short period of time is not plausible and can be accounted for by the interference of cloud coverage which interferes with the signal sent from the satellites. The shape and pattern of the low values also resemble clouds, further indicating their adverse effect on MODIS to quantify LAI. Given that the majority of trees in the tropics do not lose their leaves throughout the year, a uniform LAI raster was used for the model. This was created by taking the highest LAI values from multiple months and merging them into a single image, shown in Figure 11.

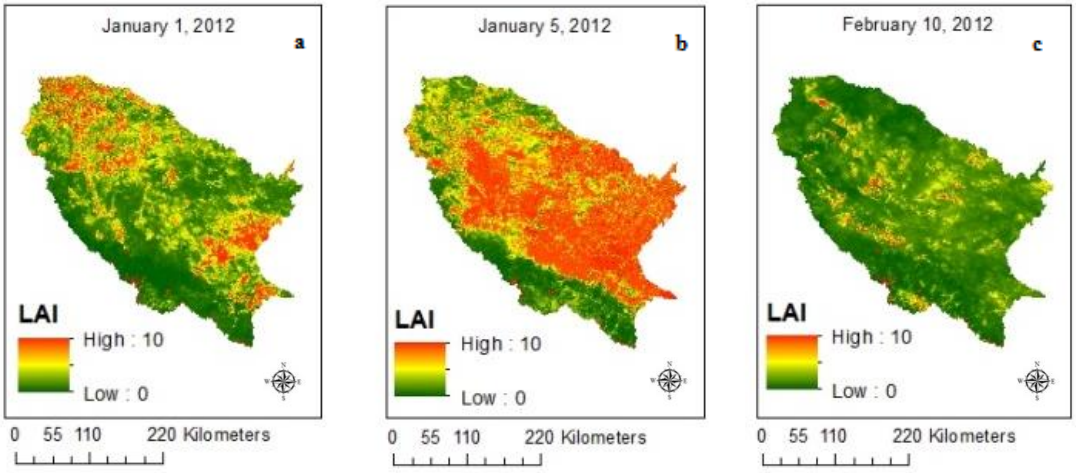

Figure 10: LAI for the Madre de Dios watershed on January 1st (a), 5th (b) and February 10th (c).

In the final LAI image, the impact from mining can be clearly seen as the Huepetuhe mine is easily visible as well as the Guacamayo and Delta 1 mines. The Andes Mountains in the Southern region of the Madre de Dios explain the low LAI values in the region. The river network is also visible as it has a slightly lower LAI value that the surrounding dense vegetation. Overall the mean LAI for the Madre de Dios Watershed is 8.1 with a standard deviation of 2.1, as seen in Table 3. This changes if the Huepetuhe sub-watershed is analyzed individually as it has a lower mean LAI of 7.7 with a higher standard deviation (STD) of 2.3.

Table 3: LAI values for the Madre de Dios Watershed as well as the Huepetuhe sub-watershed that contains the largest mine in Madre de Dios.

Watershed	Area	Mean	STD
Madre de Dios Watershed	92,263.2	8.1	2.1
Huepetuhe Watershed	1,017.9	7.7	2.3

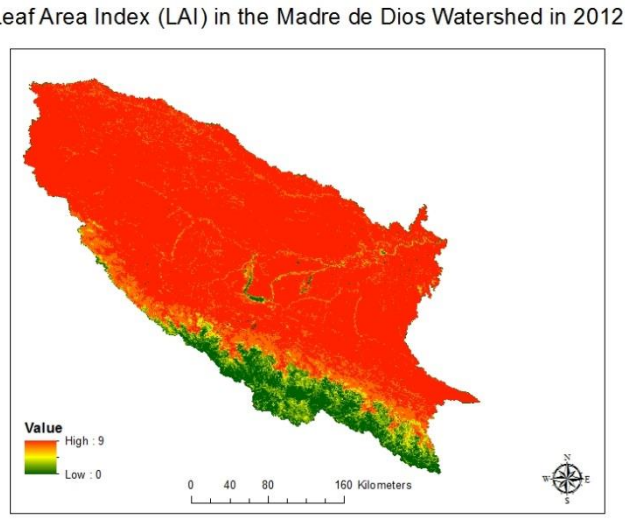

Figure 11: Yearly LAI for the Madre de Dios Watershed.

Detachment

The highest detachment rates were found in areas with steep terrain and low vegetation cover, reflected by low LAI values. Sand had the highest rates of erosion as it comprises the majority of the grain size in the steeper areas of the watershed where erosion more prevalent. The maximum(average) detachment for sand was 2,814,607 kg/m^2/year (yr) (2,137 kg/m^2/yr), while the highest rates for silt and clay were 874,883 kg/m^2/yr (416 kg/m^2/yr) and 372,901 kg/m^2/yr (258 kg/m^2/yr), respectively. The yearly detachment of sand in the watershed was found to be 220,099,000 tons, an order of magnitude higher than silt and clay, which were 42,907,000 tons and 26,587,800 tons, respectively. On a yearly basis, a total of 289,593,800 tons of soil is expected to be eroded (see Table 4). These erosion rates equate to 2,385.6 t/km^2/yr of sand, 465.1t/km^2/yr of silt and 288.2t/km^2/yr of clay, totaling 3,138.8 t/km^2/yr of soil being eroded (see Table 5).

Table 4: Yearly detachment for each grain size at the square meter scale and basin wide scale.

	Maximum Detachment Rate ($kg/m^2/yr$)	Average Detachment Rate ($kg/m^2/yr$)	Yearly detachment (tons)
Sand	2,814,607	2,137	220,099,000
Silt	874,883	416	42,907,000
Clay	372,901	258	26,587,800
Total			289,593,800

Table 5: Yearly detachment for the various grain sizes.

Erosion in the Madre de Dios Watershed	
	Erosion ($Tons/km^2/year$)
Sand	2,385.6
Silt	465.1
Clay	288.2
TOTAL	3,138.8

These results correlate well with Pelletier (2011) which found detachment rates ranging from $10t/km^2/yr$ to $10{,}000t/km^2/yr$. Unfortunately, most of the rivers in Pelletier's study that have similar measured detachment rates were in Asia and may not necessarily be comparable to the Madre de Dios Watershed. However, the model predicts erosion rates that are double those estimated elsewhere for the entire Amazon (Brown et al., 1989).

Figure 12 demonstrates that most of the erosion is from the Andes Mountains for all grain sizes, due to their steep topography and lack of dense vegetation. This is more clearly demonstrated in Figure 13, in which erosion by grain size in tons/year is shown for the entire Madre de Dios Watershed and the Huepetuhe mine. Figure 13 demonstrates that although a significant erosion rate is occurring at the Huepetuhe mine, it is a small fraction of the sediment eroded from the Andes Mountains. The subset maps in Figure 12 of the Huepetuhe mine demonstrate that higher proportions of silt and clay are being eroded due to the deforestation that has accompanied artisanal gold mining. Since the mine is located in zone 2 in the grain size distribution, it has a higher prevalence of contributing silt and clay to the environment. This is

important as mercury is known to bind onto these smaller grain sizes and become transported downriver.

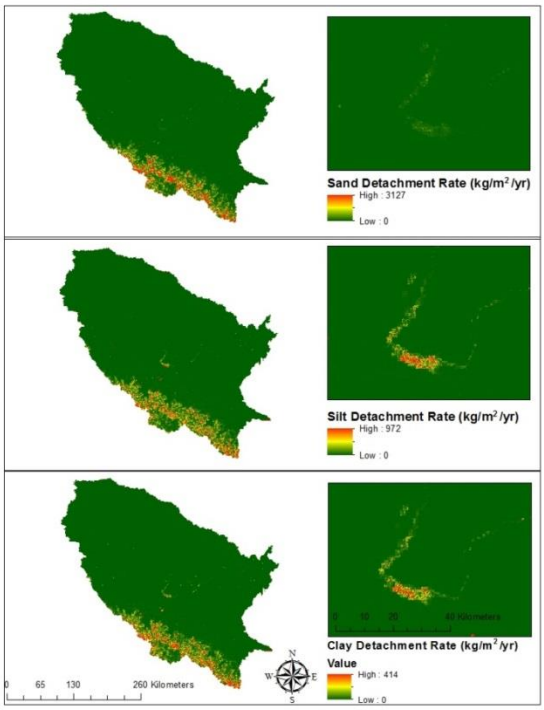

Figure 12: Yearly detachment by grain size.

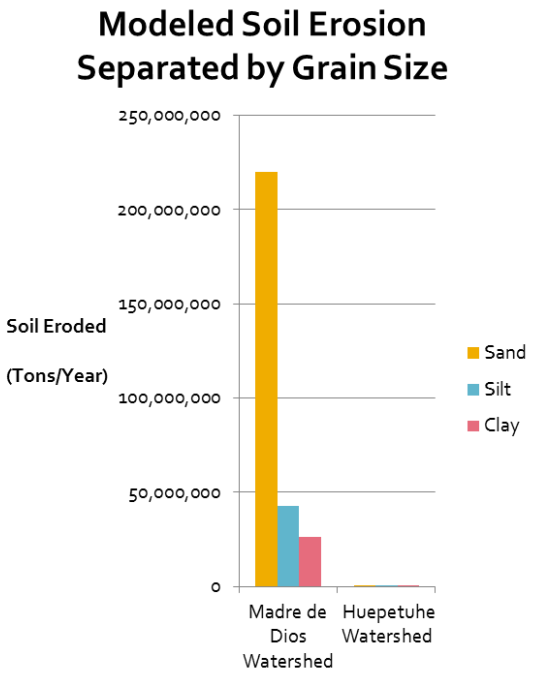

Figure 13: Soil eroded by grain size for the Madre de Dios Watershed and the Huepetuhe Watershed.

The overall impact of mining on the watershed was explored by assuming the mining areas as being covered by forest and converting their LAI values back to pre-mining conditions. The results demonstrate that mining has increased erosion by 13.1tons/km^2/yr across the entire watershed (see Table 6). The Huepetuhe, Guacamayo and Delta 1 mines are all shown to have undergone the highest increases in erosion since the establishment of artisanal gold mining (Figure14). Most of this erosion has been due to higher erosion rates of silt, which is double that of sand and clay. From this analysis, it is possible to state while mining has had a small effect on eroded volumes relative to the entire the Madre de Dios Watershed, the impact of artisanal gold mining on erosion is very significant within the Huepetuhe watershed. Erosion in tons/year of

sand, silt and clay (Figure 15 and see Table 7) before and after mining, show a drastic increase in the quantities of soil being eroded. Most of the grain sizes being eroded are those that are preferentially associated with mercury transport, of either natural or anthropogenic source. This analysis provides compelling evidence that large quantities of silt and clay are indeed made available by mining activities for mercury transport. Furthermore, if levels in the region are naturally high in mercury, this supports the hypothesis that erosion of sediment may be the main source of mercury contamination in the region.

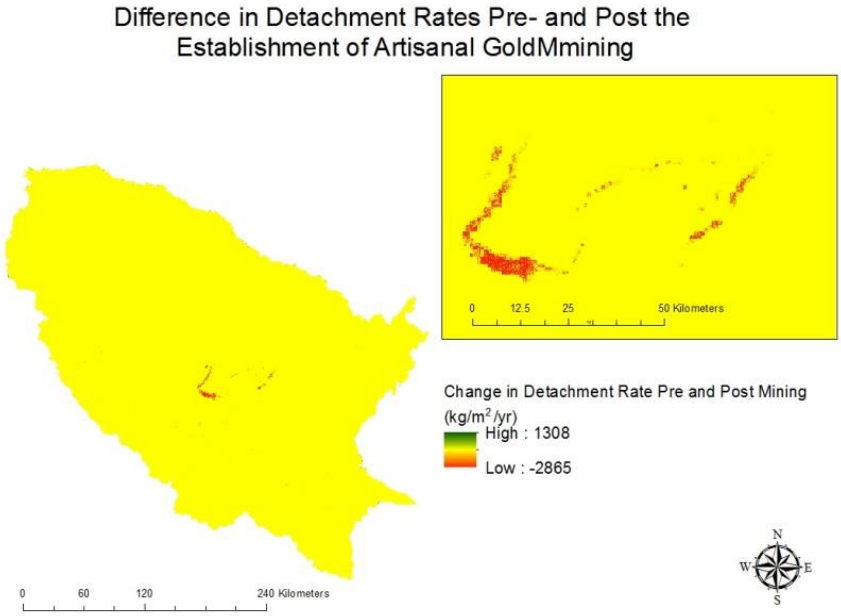

Figure 14: The difference in detachment rates before and after artisanal gold mining was established (kg/m^2/yr).

Table 6: Yearly detachment for the various grain sizes considered in the model before and after the establishment of artisanal gold mining.

Erosion in the Madre de Dios Watershed			
	Before Mining	After Mining	Difference
Sand	2,382.5	2,385.6	3.0
Silt	458.2	465.1	6.9
Clay	285.1	288.2	3.1
TOTAL	3,125.7	3,138.8	13.1
*t/km^2/yr			

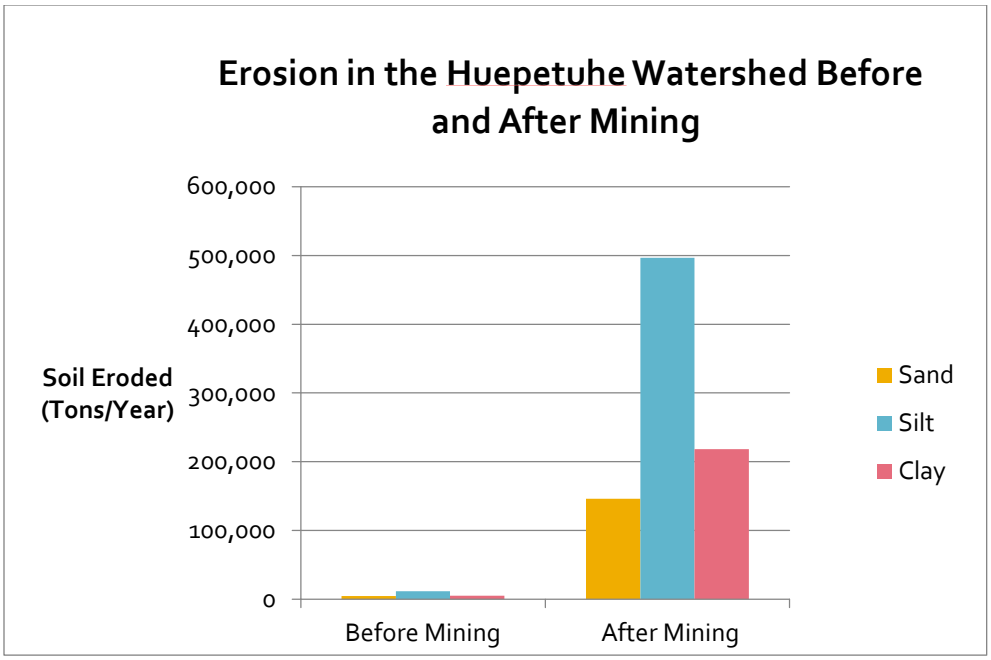

Figure 15: Soil eroded by grain size in the Huepetuhe Watershed before and after artisanal gold mining.

Table 7: Yearly detachment for the various grain sizes considered in the model before and after the establishment of artisanal gold mining in the Huepetuhe Watershed

Erosion in the Huepetuhe Watershed			
	Before Mining	After Mining	Difference
Sand	4.3	143.5	139.2
Silt	11.3	488.0	476.7
Clay	4.9	214.3	209.4
TOTAL	20.5	845.8	825.3

*t/km^2/yr

Sediment transport was also determined for the Madre de Dios watershed based on grain size (Figure 16). In order to discern differences in sediment transport an arbitrary threshold of 100,000 kg was placed to understand accumulation of each grain size (sand, silt and clay). All grain sizes are shown to quickly reach the 100,000kg threshold in the Andes Mountains, further supporting their importance as the main sediment source. However, sand (15a) does not reach the 100,000 kg threshold in the Huepetuhe or the Tambopata watersheds shown in green and red,

respectively, in 15d. This means that neither of these tributaries is contributing large amounts of sand to the Madre de Dios River. In comparison, clay and silt are major components of the Huepetuhe Watershed that are reaching the Madre de Dios River, as can be seen in 15b and 15c. While not currently an area of active mining, the model predicts that the Tambopata River, shown by the red line in 15d, is dominated by silt.

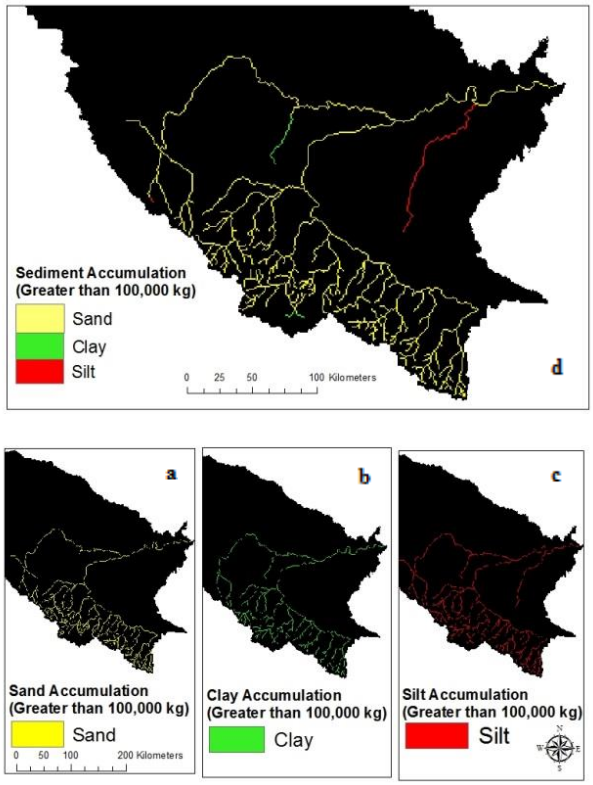

Figure 16: Sediment transport for each grain size after reaching a 100,000kg threshold, in which (a), (b), and (c) represent grain sizes sand, clay and silt, respectively. Figure 15d is a stacked image of a, b, c, from left to right.

Sediment Movement

Areas of deposition as well as transport were also modeled for the Madre de Dios Watershed; however, the constants used in Pelletier's model had to be adjusted to fit the known characteristics of the Madre de Dios. In order to do this, a nominal value for water depth for the

landscape during a rain event was estimated to be a millimeter, while the river system was estimated to have a depth of 2 meters, based on unpublished data. These values were then used to calculate a corresponding c_2 constant, using the transport equations, previously described. This modified the c_2 constant from 300 to 97 for the landscape and 0.5 for the river system, creating a more complex model for sediment transport. This provides a more realistic interpretation of potential deposition and transportation sites; however, a more complex model of the river should be constructed to predict where various grain sizes will be deposited in the river as the current model predicts that no deposition will occur in the river. The resulting deposition and transport maps for each grain size in the Madre de Dios Watershed (Figure 17) and grain sizes in the Huepetuhe Watershed (Figure 18) demonstrate that deposition and transport have an inverse relationship and that deposition increases with grain size. Sand is expected to be deposited in most regions of the Madre de Dios Watershed, except in the river system and in the steep mountainous regions. Overall, sand is expected to deposit in 87,416 km^2 and be transported in only 4,847km^2. In comparison, silt and clay are predicted to deposit in 59,884 km^2 and 40,590 km^2, respectively (See Table 8). The total area in which silt and clay can deposit is significantly less than sand, due to their slower settling velocity (W_s) causing them to be deposited farther into the Madre de Dios basin where the topography is flatter.

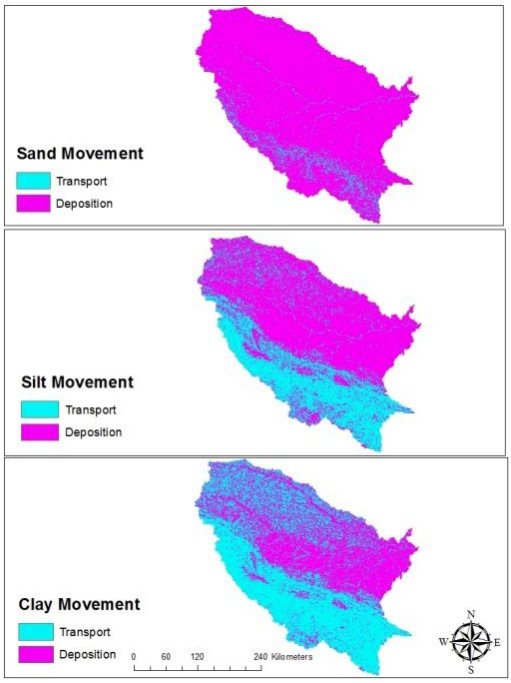

Figure 17: Sediment movement for each of the three grain sizes considered in the model. Pink areas represent areas of deposition, while light blue areas represent areas of transport.

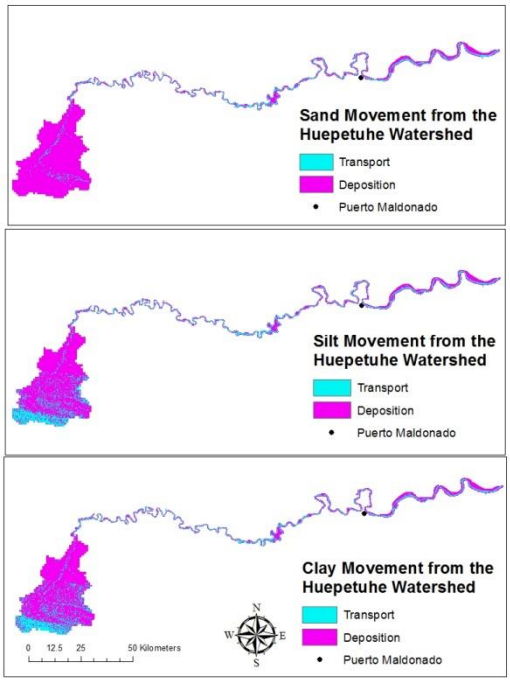

Figure 18: Sediment movement for each of the three grain sizes from the Huepetuhe Watershed to the Peruvian/Bolivian border.

Table 8: Area designated for transport or deposition for each grain size in the Madre de Dios Watershed.

Madre de Dios Watershed		
	Area of Transport (km²)	Area of Deposition (km²)
Sand	4,847.2	87,416.3
Silt	32,379.4	59,884.1
Clay	51,673.1	40,590.4

Conclusions

While one can begin to draw many interesting conclusions and hypothesis from the model, it is important to remember that a lack of data prevents a proper accuracy assessment. A consistency check with results from Pelletier (2011), as well as other models and estimates, does supports the ability of the present approach to describe sediment erosion and transport in the area. However, hard data is needed in order to better calibrate the models and understand its predictive uncertainty. More comprehensive data on the grain size fraction in the Madre de Dios would

provide an improved understanding of the abundance of grain sizes, impacting how much soil is eroded. It will also determine the extent to which naturally forming mercury is contaminating the environment through deforestation.

The application of a simple sediment detachment and transport model to the Madre de Dios Watershed allows several interesting inferences about the impact of artisanal gold mining, mercury contamination and sediment transport. The model applied here is able to define areas of deposition and transport, but a more accurate model of the Madre de Dios River must be incorporated to determine where future sediment sampling sites should be located. This is especially difficult due to the Madre de Dios River being very dynamic as it constantly forges new paths and greatly fluctuates in depth throughout the year. This entails that sites of deposition are continuously changing as well. While fine silt and clay are usually assumed to never settle due to their low settling velocity, the formation of oxbow lakes as well as of pools connected to the Madre de Dios River creates environments in which such fine grain sizes can be deposited. However, modeling where these environments will be located in such a dynamic system will be difficult.

The present analysis yields interesting suggestions on how the Madre de Dios Watershed has changed due to artisanal gold mining. While the model only describes erosion from natural processes, and neglects anthropogenic erosion, it demonstrates that deforestation alone is having substantial impacts on the Huepetuhe Watershed, causing large amounts of silt (and to a lesser extent of clay) to be eroded. Mercury is known to bind to these grain sizes, such that mercury transport is potentially promoted. While natural levels of mercury are unknown, the large amounts of silt and clay that are being eroded supports the idea that the mobilization of naturally forming mercury may be a substantial source of mercury in the Madre de Dios Watershed. However, soil tests must be done to determine actual mercury concentrations in the soil at various depths throughout the Huepetuhe Watershed to validate this hypothesis. The model results discerning areas of deposition and transport within the Madre de Dios and Huepetuhe watersheds

may locate regions where silt or clay grain sizes are more prevalent. This may be useful in arranging sampling schemes for future studies to determine mercury concentration from both natural and anthropogenic sources. This is important due to the vastness of the Madre de Dios Watershed and the limited resources to conduct such studies. If high background levels are confirmed in the soil, it would entail that the Madre de Dios Watershed is more sensitive to disturbance than previously believed and that if artisanal gold mining ceases in the region, remediation projects that incorporate re-vegetation should be implemented to reduce erosion and therefore mercury contamination.

References

Alvarez, José, Sotero, Victor, Egg, Antonio Brack, Peralta, César A. Ipenza. (2011). Minería Aurírera en Madre de Dios y contaminación con mercurio: Una bomba de tiempo. Informe preparado por el instituto de la amazonía Peruana. Lima: Peru

Ashe, Katy. (2012). Elevated Mercury Concentrations in Humans of Madre de Dios, Peru. *PLoS ONE*, 7, e3305.

Asner, Gregory P, Llactayo, William, Tupayachi, Raul, Luna, Ernesto Raez. (2013).Elevated rates of gold mining in the Amazon revealed through high-resolution monitoring. *PNAS*. Vol.110, Num.46.

Brooks, T. M., Mittermeier R. A., da Fonseca, G. A. B., Gerlach J., Hoffmann M. (2006). Global Biodiversity Conservation Priorities. *Science* 313: 58–61.

Brown, Joan, Angela, Colling, Park, Dave, Phillips, John, Rothery, Dave, Wright, John. (1989). An Introduction to Shallow-Water Environments and Their Sediments in Waves, Tides and Shallow-Water Processes. New York; Pergamon Press.

FAO/IIASA/ISRIC/ISSCAS/JRC. (2012). *Harmonized World Soil Database (version 1.2)*. FAO, Rome, Italy and IIASA, Laxenburg, Austria.

Ferguson, R. I., and M. Church. (2004). A simple universal equation for grain settling velocity. *J. Sediment. Res.*, 74, 933-937.

Forsberg, B. R., Jadim, W. F., Zeidemann, V. K., Fadini, P. S., Carneiro, A., Padovani, C. R., & Silva-Forsberg M. C. (1999). The biogeochemistry of mercury in the Negro River basin (Brazilian Amazon). Proceedings of the 5th International Conference on mercury as a Global Pollutant. Rio de Janiero:153.

Guyot, Jean Loup, Jouanneau, Jean Marie & Wasson, Jean Gabriel (1999). Characterization of river bed and suspended sediments in the Madiera drainage basin (Bolivian Amazonia). *Journal of South American Earth Sciences*. 12, 401-410.

Jardim, W. F., Fandini, P. S. (1998). Is the Negro River basin (Amazon) naturally impacted by mercury? North American Lake Management Society 18th International Symposium Banff.

Kazantzis G. (2002). Mercury exposure and early effects: an overview. *Med Lav*. 93(3), 139-147.

Knyazikhin, Y., Glassy, J., Privette, J. L., Tian, Y., Lotsch, A., Zhang… Nemani, S. W. Running, MODIS Leaf Area Index (LAI) and Fraction of Photosynthetically Active Radiation Absorbed by Vegetation (FPAR) Product (MOD15) Algorithm Theoretical Basis Document, *http://eospso.gsfc.nasa.gov/atbd/modistables.html*, 1999.

Lechler, P. J., Miller, J. R., Lacerda, L. D., Vinson, D., Bonzongo, J.-C., Lyons, W. B. & J. J. Warwick. (2000). Elevated mercury concentrations in soils, sediments, water, and fish of the Madeira River basin, Brazilian Amazon: a function of natural enrichments? *The Science of the Total Environment*, 260, 87-96.

Lucchini R, et al. (2002). Neurotoxic effect of exposure to low doses of mercury. *Med Lav*. 93(3), 202-214.

Miller, Jerry R., Orbock Miller, Suzanne M. (2007). Contaminated Rivers: A Geomorphological-Geochemical Approach to Site Assessment and Remediation. Dordrecht: Springer.

NASA Land Processes Distributed Active Archive Center (LP DAAC). (2001). ASTER L1B. USGS/Earth Resources Observation and Science (EROS) Center, Sioux Falls, South Dakota.

Pelletier, Jon D. (2011). A Spatially distributed model for the long-term suspended sediment discharge and delivery ratio of drainage basins. *Journal of Geophysical Research*. Vol. 118.

Perú Ministerio de Agricultura. (2010). Estudio Diagnóstico Hidrológico de la Cuenca Madre de Dios. Lima: Peru.

Swenson, Jennifer J., Carter, Catherine E., Domec, Jean-Christpohe, Delgado, Cesar I. (2011). Gold Mining in the Peruvian Amazon: Global Prices, Deforestation, and Mercury Imports. *PLoS ONE*. 6(4), e18875.

Thieme, Michele, Lehner, Bernhard, Abell, Robin, Hamilton, Stephen K., Kellndorfer, Josef, Powell, George, & Riveros, Juan Carlos. (2007). Freshwater conservation planning in data-poor areas: An example from remote Amazonian basin (Madre de Dios River, Peru and Bolivia). *Biological Conservation*, 135, 484-501.

Yard, Ellen E. Horton, Jane, Schier, Joshua G., Caldwell, Kathleen, Sanchez, Carlos, Lewis, Lauren & Gastanaga, Carmen. (2012) Mercury Exposure Among Artisanal Gold Miners in Madre de Dios, Peru: A Cross-sectional Study. *American College of Medical Toxicology*. Vol. 8, Num.2.

Zahir, Farhana, Rizwi, Shamim J., Haq, Soghra K., &Khan, Rizwan H. (2005) Low dose mercury toxicity and human health. *Environmental Toxicology and Pharmacology*, 20, 351-360.

Appendix

Appendix A: The monthly MODIS 15A3 HDF files used to determine LAI for the Madre de Dios Watershed

Month	MODIS15 A3 HDF Files Used for LAI
January	MCD15A3.A2012009.h10v10.005.2012017203240
January	MCD15A3.A2012013.h11v10.005.2012019051157
February	MCD15A3.A2012045.h10v10.005.2012050090304
February	MCD15A3.A2012045.h11v10.005.2012050090624
March	MCD15A3.A2012069.h10v10.005.2012075021553
March	MCD15A3.A2012073.h11v10.005.2012083005851
April	MCD15A3.A2012101.h10v10.005.2012108152523
April	MCD15A3.A2012105.h11v10.005.2012116125013
May	MCD15A3.A2012145.h10v10.005.2012153205132
May	MCD15A3.A2012145.h11v10.005.2012153205159
June	MCD15A3.A2012165.h10v10.005.2012170074508
June	MCD15A3.A2012165.h11v10.005.2012170071809
July	MCD15A3.A2012197.h10v10.005.2012202144212
July	MCD15A3.A2012197.h11v10.005.2012202144221
August	MCD15A3.A2012225.h10v10.005.2012230055638
August	MCD15A3.A2012225.h11v10.005.2012230060130
September	MCD15A3.A2012257.h10v10.005.2012262181745
September	MCD15A3.A2012257.h11v10.005.2012262181751
October	MCD15A3.A2012289.h10v10.005.2012299194100
October	MCD15A3.A2012289.h11v10.005.2012299194138
November	MCD15A3.A2012317.h10v10.005.2012322092851
November	MCD15A3.A2012317.h11v10.005.2012322095831
December	MCD15A3.A2012349.h10v10.005.2012355131354
December	MCD15A3.A2012349.h11v10.005.2012355131438

Appendix B: ASTER Global DEM data files used to determine the Madre de Dios Watershed and its slope.

ASTER Global DEM DATA Files Used for Slope
S11W070
S11W071
S11W072
S11W073
S12W069
S12W070
S12W071
S12W072
S12W073
S13W069
S13W070
S13W071
S13W072
S13W073
S14W069
S14W070
S14W071
S14W072